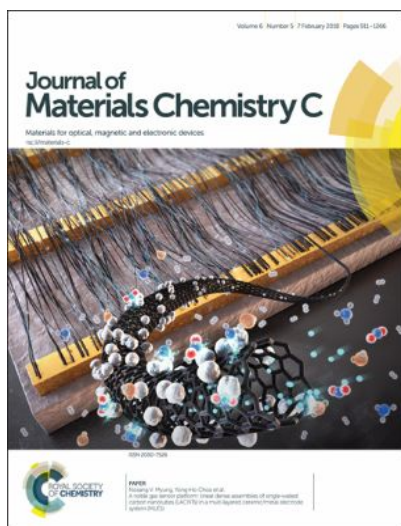




Mn²⁺-Based Narrow-Band Green-Emitting Cs₃MnBr₅ Phosphor and the performance optimization by Zn²⁺ alloying

Journal:	<i>Journal of Materials Chemistry C</i>
Manuscript ID	TC-ART-07-2019-004127
Article Type:	Paper
Date Submitted by the Author:	29-Jul-2019
Complete List of Authors:	Su, Binbin; Institute of Optical Communication Materials, South China University of Technology, State Key Laboratory of Luminescent materials and devices Molokeev, Maxim S. ; Kirensky Institute of Physics SB RAS, Xia, Zhiguo; University of Science and Technology Beijing, School of Materials Science and Engineering



Journal of Materials Chemistry C

Materials for Optical, Magnetic and Electronic Devices

Full paper submission

Journal of Materials Chemistry C is a weekly journal in the materials field. The journal is interdisciplinary, publishing work of international significance on all aspects of materials chemistry related to optical, magnetic and electronic devices. Articles cover the fabrication, properties and applications of materials.

2017 Impact Factor of *Journal of Materials Chemistry C*: **5.976**
For more information go to www.rsc.org/materialsC

The following paper has been submitted to *Journal of Materials Chemistry C* for consideration as a **Full paper**.

The Editorial Board stress a **very high quality and novelty** standard is needed for acceptance.

Journal of Materials Chemistry C wishes to publish original research that demonstrates significant **novelty and advance**, either in the chemistry used to produce materials or in the properties/applications of the materials produced. Work submitted that is outside of these criteria will not usually be considered for publication. The materials should also be related to the theme of materials for optics, magnetics and electronics.

We ask referees to examine manuscripts very carefully, and recommend rejection of articles which do not meet our high novelty, quality and impact expectations. Please note that **the rejection rate for JMC C is currently ~80%** of submitted manuscripts. **Routine or incremental** work, however competently researched and reported, should not be recommended for publication if it does not meet our expectations with regard to novelty and impact.

It is the responsibility of authors to provide fully convincing evidence for the homogeneity and identity of all compounds they claim as new. Evidence of both purity and identity is required to establish that the properties and constants reported are those of the compound with the new structure claimed.

Thank you for your effort in reviewing this submission. It is only through the continued service of referees that we can maintain both the high quality of the publication and the rapid response times to authors. We would greatly appreciate if you could review this paper in **ten days**. Please let us know if that will not be possible.

Once again, we appreciate your time in serving as a reviewer. To acknowledge this, the Royal Society of Chemistry offers a **25% discount** on its books: <http://www.rsc.org/Shop/books/discounts.asp>. Please also consider submitting your next manuscript to *Journal of Materials Chemistry C*.

Best wishes,

Dr Sam Keltie
Executive Editor
Royal Society of Chemistry

Professor Peter Skabara
Deputy Editor-in-Chief
University of Glasgow, UK

Professor Nazario Martin
Editor-in-Chief
Complutense University of Madrid, Spain



July 29, 2019

Dear editor and reviewers,

We would like to submit our manuscript entitled “**Mn²⁺-Based Narrow-Band Green-Emitting Cs₃MnBr₅ Phosphor and the performance optimization by Zn²⁺ alloying**” for your consideration as an *Article* in the *Journal of Materials Chemistry C*.

In this submission, we have discovered the novel Mn²⁺-based narrow-band green-emitting Cs₃MnBr₅ Phosphor with $\lambda_{em} = 520$ nm, FWHM = 42 nm, and the luminescence originates from the intrinsic Mn²⁺ characteristic emission with abnormal short fluorescence lifetime value in the separated [MnBr₄] tetrahedrons without concentration quenching. The thermal stability of Cs₃MnBr₅ is improved from 82% to 87% at 423 K by introducing a small amount of Zn²⁺ into Cs₃MnBr₅. By combining Cs₃Mn_{0.96}Zn_{0.04}Br₅ green phosphor, KSF:Mn⁴⁺ red phosphor and blue InGaN chips, the fabricated LED device shows the high luminous efficiency up to 107.66 lm/W with wide color gamut of 101 % NTSC for backlight display, which is larger than that of white LED based on commercial green phosphor β -SiAlON:Eu²⁺ (89%). All results indicated that Cs₃MnBr₅ and Cs₃Mn_{0.96}Zn_{0.04}Br₅ phosphors can act as a promising narrow-band emitting green phosphor in the field of wide-color-gamut LCD backlight display.

All authors have read the submitted manuscript and approve of its submission. Thank you very much for your consideration.

Sincerely,

Zhiguo Xia

Professor of Materials Chemistry and Physics

State Key Laboratory of Luminescent Materials and Devices and Institute of Optical Communication
Materials, South China University of Technology, Guangzhou, 510641, China
Email: xiazg@scut.edu.cn, Tel.: + 86-13810670492



Mn²⁺-Based Narrow-Band Green-Emitting Cs₃MnBr₅ Phosphor and the performance optimization by Zn²⁺ alloying[†]

Received 00th January 20xx,

Binbin Su,^a Maxim Molochev^{cde}, Zhiguo Xia ^{*a}

Accepted 00th January 20xx

DOI: 10.1039/x0xx00000x

To discover new narrow-band green-emitting phosphors is a challenge for backlighting light-emitting diodes (LEDs) used in liquid crystal displays (LCDs). The synthesis and optical properties Cs₃MnBr₅ is demonstrated, and the intrinsic Mn²⁺ luminescence leads to intense green emission at 520 nm with narrow full width at half maximum of 42 nm and high photoluminescence quantum yield (PLQY) of 49% under the excitation at 460 nm. When a small amount of Zn²⁺ is introduced into Cs₃MnBr₅, the luminescence intensity decreased slightly, moreover, the thermal stability of Cs₃MnBr₅ is improved from 82% to 87% with the intensity values at 423 K compared to that at 298 K. The white LED device fabricated by Cs₃Mn_{0.96}Zn_{0.04}Br₅ (green) and K₂SiF₆:Mn⁴⁺ (red) phosphors with a blue LED chip exhibit a high luminous efficiency (107.76 lm W⁻¹) and wide color gamut (101% National Television System Committee standard (NTSC) in Commission Internationale de L'Eclairage (CIE) 1931 color space), demonstrating its potential application in wide color gamut LCD backlight.

1. Introduction

Phosphor-converted light-emitting diode (LED) based on a blue-emitting GaN chip acts as a new backlight technology, which has been widely used in modern liquid crystal displays (LCDs) owing to its spectral adjustability, stability and high light efficiency, etc.¹⁻³ In this technique, phosphors, work as the key materials, the luminescent properties, such as peak position and full-width at half-maximum (FWHM) of green and red emitters significantly affect the gamut range, color purity, luminescence efficiency and reliability of backlight unit.^{4, 5} Therefore, it is crucial to develop narrow-band green or red phosphors in suitable spectral region to enlarge the maximum accessible color gamut and color purity, and increase the visual luminous efficacy for extending the practical application. Since the human eyes are able to clearly distinguish green light, thus, the discovery of highly efficient narrow-band green-emitting phosphors seem to be particularly important. In the typically commercial wide gamut LED backlight devices, the narrow-band green-emitting phosphor, β-SiAlON:Eu²⁺ with the emission peaking at 540 nm is considered as the optimum choice.⁶ Although the luminescence properties of β-SiAlON:Eu²⁺ significantly improved, the narrowest one also limits the maximum accessible color gamut of backlighting display application (90% of NTSC) due to unsatisfied FWHM.⁷

Recently, various green-emitting materials in different systems have been developed. In particular, the perovskite CsPbBr₃ quantum dots (QDs) were emerged as the green phosphors in wide-color gamut backlight display due to their high PLQYs, and superior narrow emission bands with an FWHM of only ≈ 20 nm. The White LED fabricated with green phosphor mesoporous-CsPbBr₃/SDDA@PMMA, red phosphor KSF:Mn⁴⁺ and blue LED chip, exhibits high color-gamut with 102% of NTSC. However, the unstable PLQY caused by poor stability and the degradation behavior in the ambient environment are the achilles heel, restricting their commercial applications, although a variety of methods have been used to modify their deficiencies.⁸⁻¹⁰ On the contrary, other inorganic green phosphors beyond β-SiAlON:Eu²⁺ also exhibit high luminescence efficiency, moisture resistance, and excellent thermal stability in this application. Xie et al. reported Ba₂LiSi₇AlN₁₂:Eu²⁺ and Ba[Li₂(Al₂Si₂)N₆]:Eu²⁺ green phosphors peaked at ≈ 515 nm, 532 nm with an FWHM of 61 nm, 57 nm respectively, however, they are still difficult to satisfy the maximum accessible color gamut of backlights due to the unmatched FWHM, peak position, and the harsh synthesis condition also restrict the application.^{11, 12} Recently, our group discovered several novel UC₄C₄-related narrow-band green-emitting phosphors, in which RbLi(Li₃SiO₄)₂:Eu²⁺ showed a green emission at 530 nm with a narrow FWHM of 42 nm, and an NTSC value of 107%. To further optimize the luminescence properties and improve the stability, the Na⁺ were substituted for Li⁺, the green emission of RbNa(Li₃SiO₄)₂:Eu²⁺ was obtained with the emission peaking at 523 nm and FWHM of 41 nm, meanwhile, the color gamut of WLED were improved from 107% to 113 % NTSC, and the chemical stability has been improved.^{13, 14} In addition to CsPbBr₃ perovskite QDs and rare earth Eu²⁺ doped green emitting phosphors, transition metal Mn²⁺ activated green phosphors can also show potential application in LED backlight. For example, γ-AION:Mn²⁺, Mg²⁺ exhibits a FWHM of 44

^a State Key Laboratory of Luminescent Materials and Devices and Institute of Optical Communication Materials, South China University of Technology, Guangzhou 510641, China.

^b Laboratory of Crystal Physics, Kirensky Institute of Physics, Federal Research Center KSC SB RAS, Krasnoyarsk 660036, Russia

^c Siberian Federal University, Krasnoyarsk 660041, Russia

^d Department of Physics, Far Eastern State Transport University, Khabarovsk 680021 Russia

[†] Electronic supplementary information (ESI) available.

nm with color gamut of 102% NTSC, and $\text{MgAl}_2\text{O}_4:\text{Mn}^{2+}$ with a FWHM of 35 nm, color gamut of 116% NTSC. Moreover, $\text{Sr}_2\text{MgAl}_{22}\text{O}_{36}:\text{Mn}^{2+}$ phosphor has narrow FWHM with 26 nm and wide color gamut with 127% of NTSC. For $\text{ZnAl}_2\text{O}_4:\text{Mn}^{2+}$, the FWHM can be even tuned to 18 nm.¹⁵⁻¹⁸ However, the emission of Mn^{2+} belong to the spin-forbidden d–d transition from ${}^4\text{T}_1$ excited state to ${}^6\text{A}_1$, thus, Mn^{2+} -doped green phosphors generally have low absorption efficiency or the quantum efficiency, moreover, the long fluorescence lifetime compared with rare earth Eu^{2+} doped phosphors will restrict the application.

As mentioned above, perovskite QDs possess the characteristic narrow-band emission, but lack of high physicochemical stability due to the existence of intrinsic defect; while inorganic phosphors normally show excellent stability, but are unsatisfied with the FWHM of the emission band. Therefore, the discovery of physicochemical stability and efficient narrow-band green-emitting phosphors are urgent. In this paper, we develop a new Mn^{2+} -based narrow-band green-emitting phosphor Cs_3MnBr_5 with intrinsic Mn^{2+} emission, which can be irradiated effectively by blue LED chip and shows a narrow band (FWHM = 42 nm) green emission peaking at 520 nm with high PLQYs (49 %) and a relative short fluorescence lifetime of 0.29 ms. The luminescence intensity of Cs_3MnBr_5 almost retain unchanged in low Zn^{2+} doped concentrations. It's worth noting that after doping 4% Zn^{2+} into Cs_3MnBr_5 , the thermal stability is obviously improved from 82 to 87 % with the intensity values at 423K compared to that at 298 K. In addition, the white LED device fabricated by Cs_3MnBr_5 (green) and $\text{K}_2\text{SiF}_6:\text{Mn}^{4+}$ (red) phosphors with a blue LED chip was obtained with high efficiency (108.88 lm W^{-1}) and wide color gamut (104% NTSC). After doping 4% Zn^{2+} into Cs_3MnBr_5 , the stability of white LED device fabricated with $\text{Cs}_3\text{Mn}_{0.96}\text{Zn}_{0.04}\text{Br}_5$ green phosphor are improved compared with undoped one, which indicated that $\text{Cs}_3\text{Mn}_{0.96}\text{Zn}_{0.04}\text{Br}_5$ has potential as green-emitting phosphors for backlighting display applications.

2. Experimental section

2.1 Materials and Preparation

The polycrystalline samples of Cs_3MnBr_5 and Zn^{2+} -doped Cs_3MnBr_5 were synthesized by evaporative crystallization with stoichiometric amount of Cs_2CO_3 (99.99%, Aladdin), MnCO_3 (99.95%, Aladdin), ZnO (99.99%, Aladdin). In a typical procedure of Cs_3MnBr_5 , 1.5 mmol Cs_2CO_3 and 1 mmol MnCO_3 were dissolved in a desired amount of the HBr. After the dissolution of reactant, excess acid was boiled off and the solutions were evaporated to dryness. The obtained sample were dissolved in adequate ethyl alcohol to washing superfluous impurity. Finally, the obtained products was dried at 373 K for 2 h in air.

2.2 Fabrication of PC-LEDs

The white LEDs were fabricated by integrating the Cs_3MnBr_5 or $\text{Cs}_3\text{Mn}_{0.96}\text{Zn}_{0.04}\text{Br}_5$ green phosphor, the $\text{KSF}:\text{Mn}^{4+}$ commercial red phosphor (Beijing Yuji Science & Technology Co., Ltd, China) and blue LED InGaN chips (450-460 nm, 2.7–3.4 V, 300 mA, Shenzhen VANDO Technology Co., Ltd, China). The phosphors were thoroughly mixed with epoxy resin, and the obtained mixture was coated on the LED chips. The photoelectric properties, such as, the emission spectrum, color temperature (CCT), color rendering index (Ra) and CIE color

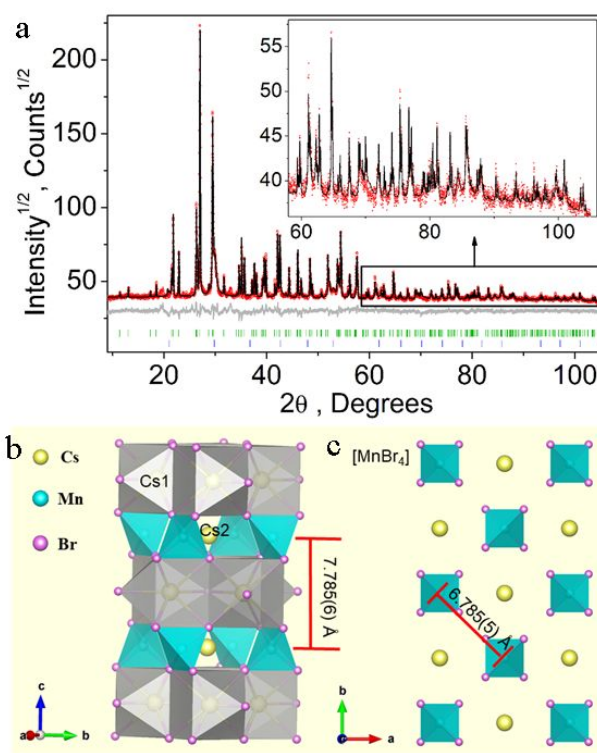


Fig.1 (a) The Rietveld refinement XRD patterns of Cs_3MnBr_5 . (b) Crystal structure of Cs_3MnBr_5 . (c) Inside the ab plane, the distance between two nearest manganese bromide tetrahedrons.

coordinate of the LED, were collected by using an integrating sphere spectroradiometer system (ATA-1000, Ever fine).

2.3 Characterization

Structural characterization was conducted by using an Aeries powder X-ray diffraction (XRD) diffractometer (PANalytical Corporation, Netherlands) operating at 40 kV and 40 mA with monochromatized Cu K α radiation ($\lambda = 1.5406 \text{ \AA}$). The data used for Rietveld analysis (2θ range $10\text{--}105^\circ$) was collected in a step-scanning mode with a step size of 0.01° and 10 s counting time per step. The Rietveld structure refinements were performed by using TOPAS 4.2. The electron paramagnetic resonance (EPR) spectroscopy were recorded by an electron paramagnetic resonance EPR spectrometer (Bruker, A300). The room-temperature photoluminescence (PL) and photoluminescence excitation (PLE) spectra were carried out in a FLS920 fluorescence spectrophotometer (Edinburgh Instruments Ltd., U.K.) with the Xe900 lamp as the excitation source. The same instrument was used to collect the decay data with a μF900 lamp used as the excitation source. Temperature-dependent PL spectra measurement were conducted by a fluorescence spectrophotometer (F-4600, HITACHI, Japan), and the phosphor powders were heated to 523 K in a 25 K interval at a heating rate of 100 K min^{-1} and held at each temperature for 10 min for thermal equilibrium. The PLQYs was measured by a Quantaurus-QY spectrophotometer equipped with an integrating sphere (Hamamatsu Photonics, Japan).

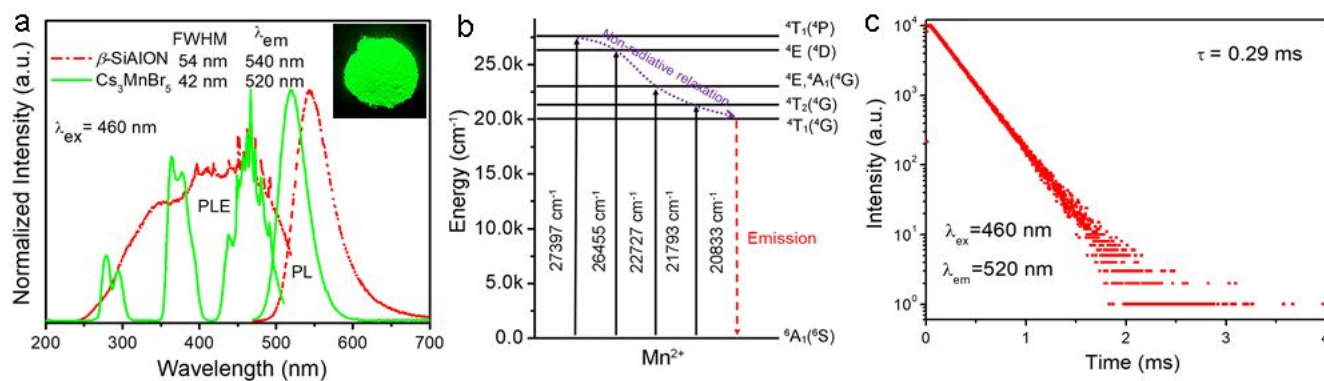


Fig.2 (a) PLE and PL spectra of Cs₃MnBr₅ (green solid line) and β -SiAlON (red dotted line). The insets show the digital photographs of green Cs₃MnBr₅ phosphor under 365 nm UV lamp. (b) The decay curve of Cs₃MnBr₅ under excitation at 460 nm, monitored at 520 nm. (c) The Schematic diagram showing the energy adsorption, non-radiative relaxation, and emission process of Mn²⁺ in a tetrahedral environment.

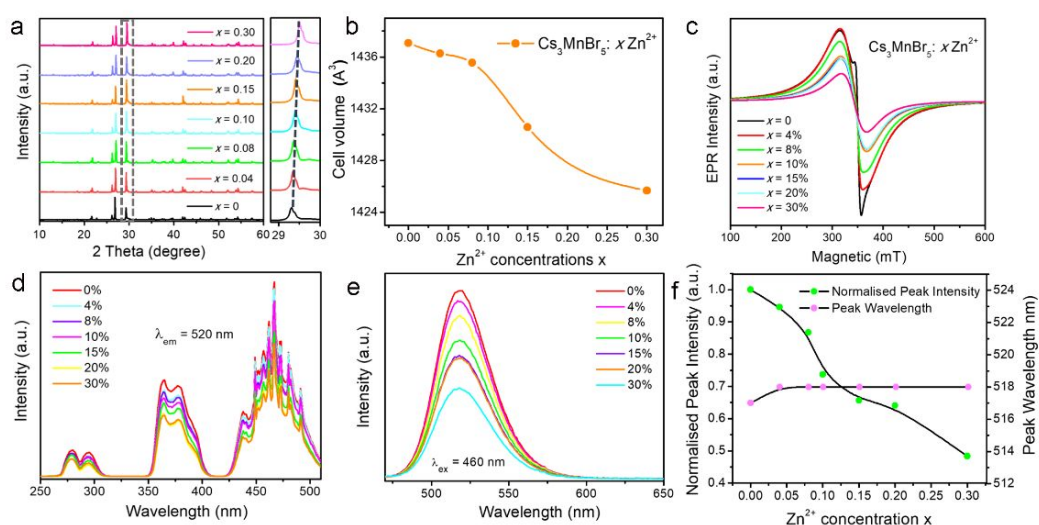


Fig. 3. (a) XRD pattern of Cs₃Mn_{1-x}Br₅: xZn²⁺ (x = 0 - 0.30). (b) The variation of Cell volume of Cs₃MnBr₅: xZn²⁺ (x = 0.04, 0.08, 0.15, 0.30). (c) EPR spectra of Zn²⁺-doped Cs₃MnBr₅ obtained with different Zn²⁺: Mn²⁺ ratios. The PLE (d) and PL (e) spectra of Cs₃MnBr₅: xZn²⁺ (x = 4%, 8%, 10%, 15%, 20%, 30%). (f) The intensity and wavelength change of emission peak of different doping concentration of Zn²⁺.

3 Results and discussion

3.1 Phase Formation

The phase purity of the as-prepared Cs₃MnBr₅ powders was investigated by the X-ray powder diffraction (XRD) measurement. Profile fitting via the Rietveld method was carried out for Cs₃MnBr₅ (Fig. 1a) by using TOPAS 4.2.¹⁹ All peaks were indexed by tetragonal unit cell with parameters highly consistent with the reported pattern of Cs₃MnBr₅ (PDF card No.71-1416), therefore this structure was taken as starting model for Rietveld refinement. The refinement result shows that this phase has a tetragonal unit cell of $a = b = 9.60672$ (13) Å, $c = 15.5716$ (2) Å, and $V = 1437.08$ (4) Å³. Refinement was stable and gave low R-factors, and the detailed information of the refinement processing are provided in Table S1, S2, S3. The as-prepared Cs₃MnBr₅ belong to the tetragonal system, space group 14/mcm, isostructural with Cs₃CoCl₅. In this structure, Mn²⁺ (4b) site is bonded to four bromine atoms form [MnBr₄] regular tetrahedron geometry with D_{2d} symmetry. Cs2 (4a) sites coordinate with ten bromine atoms form distorted [CsBr₁₀] polyhedrons, which share two

Br1 anions with [MnBr₄] tetrahedrons result in independent distribution of [MnBr₄] tetrahedrons (Fig. 1b). The Cs1 (8h) sites coordinate with eight bromine atoms form distorted [CsBr₈] polyhedrons, which are linked with each other by faces and form ...-[CsBr₈]-[CsBr₈]-... layer. [MnBr₄] tetrahedrons are share two Br1 anion with [CsBr₈] polyhedrons form an alternating layer structure. Mn²⁺ (4b) site in Cs₃MnBr₅ are layer distributed along the c-axis direction, the neighbouring manganese bromide tetrahedrons are separated by cesium bromide polyhedrons and keep a distance of 7.785 (6) Å. Inside the *ab* plane, the distance between two nearest manganese bromide tetrahedrons, with the value of approximately 6.785(5) Å (Fig. 1c). To investigate the thermal stability of Cs₃MnBr₅, thermo-gravimetric analysis (TGA) was carried out from room temperature to 923 K, and the mass-change curve was show in Fig. S1. The sample exhibit good thermal stability up to T = 723 K. The decomposition of sample mainly was divided into two steps. In the first stage (298 - 423 K), the quality of Cs₃MnBr₅ was lost 3.76 % due to the evaporation of crystal water. The second stage (728 - 923 K)

ARTICLE

Journal Name

was the process where the metal (II) bromide decomposed continuously.

The PLE and PL spectra of Cs_3MnBr_5 phosphor with intrinsic Mn^{2+} emission were shown in Fig. 2a. The excitation spectrum exhibit structured bands with three maxima at 278, 365, and 460 nm,

Table 1 The comparisons of fluorescence lifetime of green phosphors and luminous efficiency of WLED devices

Green phosphors	Lifetime	luminous efficiency (with KSF: Mn^{2+})	Ref
$\beta\text{-SiAlON}:\text{Eu}^{2+}$	1 μs	136 lm/w	[7]
RLSO: Eu^{2+}	0.84 μs	97.28 lm/w	[13]
$\gamma\text{-AlON}:\text{Mn}^{2+}, \text{Mg}^{2+}$	3.89 ms	-	[15]
$\text{MgAl}_2\text{O}_4:\text{Mn}^{2+}$	6.51 ms	56.32 lm/w	[23]
$\text{Sr}_2\text{MgAl}_{22}\text{O}_{36}:\text{Mn}^{2+}$	4.71 ms	70.58 lm/w	[17]
Cs_3MnBr_5	0.29 ms	108.88 lm/w	This work
$\text{Cs}_3\text{Mn}_{0.96}\text{Zn}_{0.04}\text{Br}_5$	0.30 ms	107.76 lm/w	This work

corresponding to the electronic transitions of Mn^{2+} in $[\text{MnBr}_4]$ tetrahedra from the ${}^6\text{A}_1$ ground state to T_d excited states due to the energy splitting in the ${}^4\text{T}_1$ excited state with D_{2d} symmetry (Fig. 2a). The intense band centred at 278 nm together with two main absorption peaks at 350 and 460 nm, indicating Cs_3MnBr_5 phosphor can be excited by UV and blue LED chips. Under the excitation at 460 nm, Cs_3MnBr_5 shows a prominent green emission at 520 nm with FWHM of 42 nm with the high PLQY of 49%. The as-prepared powder also exhibits an intense green light under 365 nm lamp irradiation, as shown in the inset (Fig. 2a). The strong green emission is ascribed to the metal-centred d-d transition of the Mn^{2+} ion in d^5 configuration with a tetrahedral coordination geometry.²⁰ The detailed energy absorption, non-radiative relaxation, and emission process of Mn^{2+} in a tetrahedral environment were described in Fig. 2b. The decay curve of Cs_3MnBr_5 phosphor under excitation at 460 nm, monitored at the peak of 520 nm at room temperature is presented in Fig. 2c. The decay curve can be fitted using a single exponential decay formula:²¹

$$I(t) = I_0 + A \exp\left(-\frac{t}{\tau}\right) \quad (1)$$

Where $I(t)$ and I_0 are the luminescence intensity at time t and $t \gg \tau$, A is a constant, and τ is the decay time for an exponential component. As shown in Fig. 2c, by using the above fitting equation, the fluorescence lifetime for Cs_3MnBr_5 is determined to be 0.29 ms. The single exponential decay behaviour also confirms the unique Mn^{2+} site in Cs_3MnBr_5 phosphor.

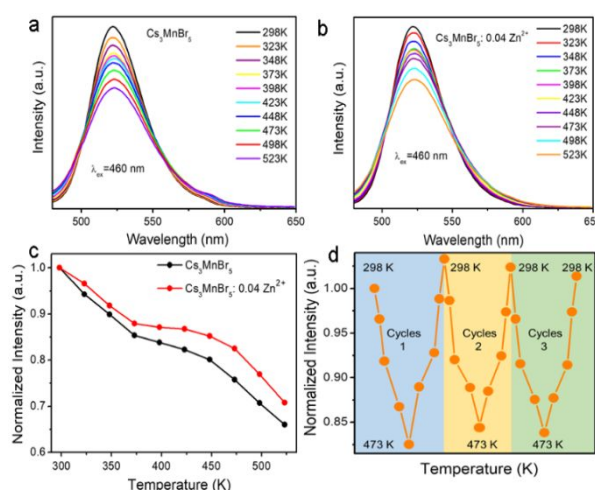


Fig. 4. Temperature-dependent PL spectra of Cs_3MnBr_5 (a) and $\text{Cs}_3\text{Mn}_{0.96}\text{Zn}_{0.04}\text{Br}_5$ (b) under 460 nm excitation in the temperature range of RT–523 K with a temperature interval of 298 K. (c) Temperature-dependent normalized integrated PL intensities of Cs_3MnBr_5 and $\text{Cs}_3\text{Mn}_{0.96}\text{Zn}_{0.04}\text{Br}_5$. (d) The corresponding emission intensity with three heating and cooling cycles of the $\text{Cs}_3\text{Mn}_{0.96}\text{Zn}_{0.04}\text{Br}_5$ phosphor from 298 to 473 K.

To prove potential application of Cs_3MnBr_5 , The $\beta\text{-SiAlON}:\text{Eu}^{2+}$ green phosphor was chosen as a reference to compare the optical performance. The dashed dotted red lines in Fig. 2a show the PLE and PL spectra of $\beta\text{-SiAlON}:\text{Eu}^{2+}$, which can be excited by UV to blue light and shows a narrow-band emission at 540 nm with FWHM of 54 nm under 460 nm excitation.⁷ Obviously, the PL spectrum of Cs_3MnBr_5 is narrower than that of $\beta\text{-SiAlON}:\text{Eu}^{2+}$ with more proper emission peak (520 nm) for LCD applications, suggesting that Cs_3MnBr_5 is more suitable for wide color gamut display backlights. Generally, the narrower FWHM implies higher color purity (CP), therefore, the comparison of CP between Cs_3MnBr_5 and the commercial $\beta\text{-SiAlON}:\text{Eu}^{2+}$ phosphors are also studied. The CIE coordinations of the Cs_3MnBr_5 and $\beta\text{-SiAlON}:\text{Eu}^{2+}$ phosphors are calculated to be (0.1490, 0.7564) and (0.2405, 0.6312), respectively. The CIE diagram is encircled by monochromatic color coordinates from 380 to 700 nm. The color purity of a specific color is defined by the percentage of the linear distance between the chromaticity coordinates of the sample emission and the CIE1931 standard source to the linear distance between the chromaticity coordinates of the monochromatic light source and the standard source, which can be calculated by the following equation:²²

$$\text{color purity} = \frac{\sqrt{(x-x_i)^2 + (y-y_i)^2}}{\sqrt{(x_d-x_i)^2 + (y_d-y_i)^2}} \times 100\% \quad (2)$$

where (x, y) represents the CIE color coordination of the Cs_3MnBr_5 and $\beta\text{-SiAlON}:\text{Eu}^{2+}$ phosphors, (x_i, y_i) stand for the CIE1931 standard source with CIE color coordinate (0.3333, 0.3333), and (x_d, y_d) is the color coordinate corresponding to the monochromatic light source. The CP of the Cs_3MnBr_5 and $\beta\text{-SiAlON}:\text{Eu}^{2+}$ phosphors were calculated to be 78.98% and 59.12%, respectively. The higher CP of Cs_3MnBr_5 phosphor will help to achieve larger color gamut for backlighting LEDs.

In addition, for phosphors applied to LCD display, long decay time will generate ghost signal, which severely affects the visual

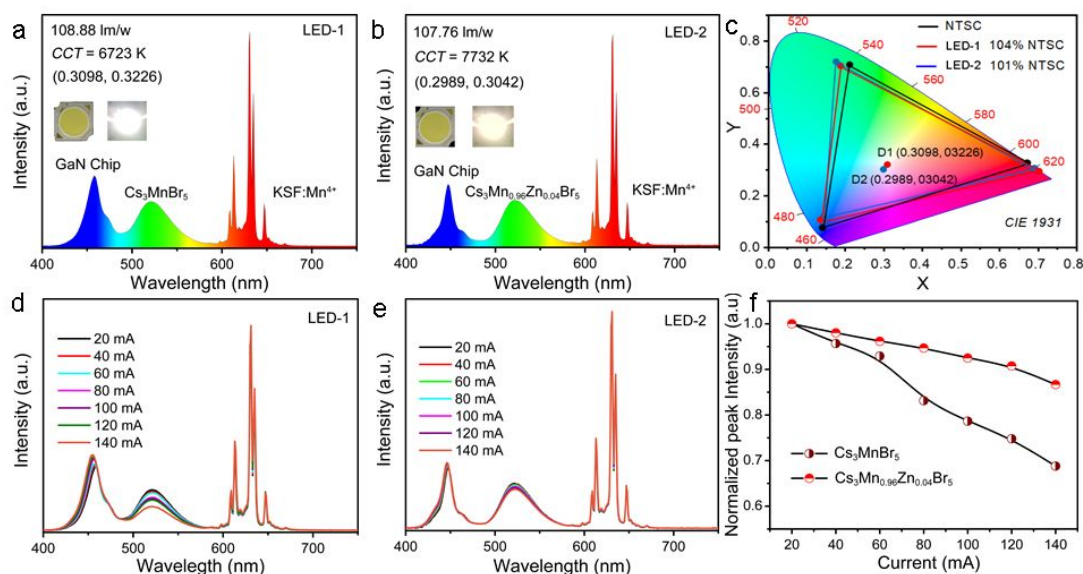


Fig 5. (a, b) PL spectrum of the WLED devices fabricated with the green phosphor Cs_3MnBr_5 , $\text{Cs}_3\text{Mn}_{0.96}\text{Zn}_{0.04}\text{Br}_5$ and the commercial red phosphor $\text{KSF}:\text{Mn}^{2+}$ on a blue LED GaN chip under a current of 20 mA respectively. The inset shows the photographs of the as-fabricated and lightened LEDs. (c) CIE 1931 color coordinates of fabricated LEDs, and color space of NTSC standard (red line) and LED-1 (black line) and LED-2 (blue line). (d, e) PL spectra of the fabricated LEDs under various operating currents. (f) The peak intensity variation of green phosphors in WLEDs under various operating currents.

effect when watching high definition programs. The comparison of the fluorescence lifetime among the well-known green phosphors are listed in Table 1. The microsecond range of fluorescence lifetime (0.29 ms) of Mn^{2+} in Cs_3MnBr_5 is more shorter than that Mn^{2+} -doped $\text{MgAl}_2\text{O}_4:\text{Mn}^{2+}$, $\gamma\text{-AlON}:\text{Mn}^{2+}, \text{Mg}^{2+}$ and $\text{Sr}_2\text{MgAl}_{22}\text{O}_{36}:\text{Mn}^{2+}$ green phosphors with 6.51, 3.89 and 4.71 ms, respectively.^{15, 17, 23} The abnormal character with short lifetime value should be related with the intrinsic Mn^{2+} emission in Cs_3MnBr_5 , and the $[\text{MnBr}_4]$ tetrahedrons are separated each other. Moreover, the fluorescence lifetimes of Mn^{2+} is only two orders of magnitude difference from that of the Eu^{2+} -doped green phosphors. In other words, the transition metal Mn^{2+} -doped green phosphors with short fluorescence lifetime is more expected to achieve broader application in backlighting LEDs.

In order to study the effect of Mn^{2+} concentration on the luminescence properties of Cs_3MnBr_5 , the Zn^{2+} was introduced into Cs_3MnBr_5 to substitute Mn^{2+} partially. The typical XRD patterns of $\text{Cs}_3\text{MnBr}_5:\text{xZn}^{2+}$ samples for various Zn^{2+} concentrations are shown in Fig. 3a. The results indicate that all the diffraction peaks of the as-prepared $\text{Cs}_3\text{MnBr}_5:\text{xZn}^{2+}$ ($4 \leq x \leq 30\%$) samples can match well with the standard Cs_3MnBr_5 data (PDF card No.71-1416), and there are no impurity phases with the increase of Zn^{2+} concentration (x). The slightly shift of diffraction peaks (right part of Fig. 3a) as well as the diminution of cell volume (Fig. 3b) are in a good agreement with the fact that the radius of Zn^{2+} is smaller than that of Mn^{2+} . In addition, the decrease of EPR signal of the Cs_3MnBr_5 further verify the successful doping of Zn^{2+} ion (Fig. 3c). The PLE and PL spectra of the $\text{Cs}_3\text{MnBr}_5:\text{xZn}^{2+}$ ($4 \leq x \leq 30\%$) samples are described in Fig. 3d,e. The PL intensity gradually decreased with the increase of Zn^{2+} concentration, in addition, both the position and FWHM of emission band almost remain unchanged (Fig. 3f), which indicated that there is no concentration quenching in Mn^{2+} -based Cs_3MnBr_5 phosphor. As mentioned above, in Cs_3MnBr_5 , the shortest distance between two

Cesium bromide polyhedrons are 6.785 (5) Å, the inter- and intralayer far distances of cesium bromide polyhedrons will restrict the direction of energy migration result in high luminescence efficiency without concentration quenching.²⁴

The thermal stability of phosphors has an important effect on various performance parameters of the corresponding device.²⁵ Thus, temperature is a critical parameter to evaluate the potential application of phosphors. Fig. 4a,b comparatively shows the temperature-dependent PL spectra of Cs_3MnBr_5 and $\text{Cs}_3\text{Mn}_{0.96}\text{Zn}_{0.04}\text{Br}_5$ phosphors from room temperature (RT, 298K) to 523K with a step interval of 25K. With the increasing of temperature, the emission intensity gradually decreases, which caused by nonradiative transitions due to the lattice vibration and the lattice relaxation of the luminescent centres.¹⁷ The comparison of integrated PL intensities between Cs_3MnBr_5 and $\text{Cs}_3\text{Mn}_{0.96}\text{Zn}_{0.04}\text{Br}_5$ from 298 to 523 K are shown in Fig. 4c. The Cs_3MnBr_5 presents a relatively low luminescence quenching behaviour with integrated PL intensities remain 82% at 423 K of the initial intensity measured at 298 K. Moreover, integrated PL intensities of $\text{Cs}_3\text{Mn}_{0.96}\text{Zn}_{0.04}\text{Br}_5$ can still remain 87% at 423 K, which indicated that the doping Zn^{2+} into Cs_3MnBr_5 effectively improve the thermal stability. The tendencies of integrated PL intensities with three heating and cooling cycles of the $\text{Cs}_3\text{Mn}_{0.96}\text{Zn}_{0.04}\text{Br}_5$ from 298 to 473 K also has been investigated and are shown in Fig.4d. After three cycles of heating and cooling process, the thermal stability of $\text{Cs}_3\text{Mn}_{0.96}\text{Zn}_{0.04}\text{Br}_5$ almost remain unchanged, the integrated PL intensity even have slightly promotion after cool to room temperature. All of results indicate that $\text{Cs}_3\text{Mn}_{0.96}\text{Zn}_{0.04}\text{Br}_5$ phosphor possesses better temperature-dependent stability, so that it can play a key role in the green phosphor in backlighting display.

Considering the practicability of synthesized phosphors in wide color gamut display backlights, the LEDs integrated with green

phosphor Cs_3MnBr_5 or $\text{Cs}_3\text{Mn}_{0.96}\text{Zn}_{0.04}\text{Br}_5$, red phosphor $\text{K}_2\text{SiF}_6:\text{Mn}^{4+}$, and commercial blue emitting InGaN chips were fabricated, which are denoted as LED-1 (Cs_3MnBr_5) and LED-2 ($\text{Cs}_3\text{Mn}_{0.96}\text{Zn}_{0.04}\text{Br}_5$). The PL spectra of the fabricated LED devices under a current of 20 mA are shown in Fig. 5a,b, the inset shows the photographs of the LED devices. The LED-1 and LED-2 shows a bright white light with a high luminous efficiency up to 108.88 lm/W and 107.76 lm/W, which are higher than other previous reported phosphor-converted WLEDs (Table 1), except for the recently reported $\beta\text{-SiAlON}:\text{Eu}^{2+}$ based WLED. The calculated color gamut cover the color space of the 104% and 101% in CIE 1931 with CIE color coordinate is (0.3098, 0.3226) and (0.2989, 0.3042), respectively. Fig. 5d,e show the PL spectra of the fabricated LEDs under the various operating currents. Compared with LED-1, the LED-2 exhibits better stability, the PL intensity of $\text{Cs}_3\text{Mn}_{0.96}\text{Zn}_{0.04}\text{Br}_5$ still retain 86% at 140 mA operating currents (Fig.5f). The results demonstrate that the introduction of Zn^{2+} into Cs_3MnBr_5 significantly improved the stability of LED device. $\text{Cs}_3\text{Mn}_{0.96}\text{Zn}_{0.04}\text{Br}_5$ is being looked at broadly for potential applications in LCD backlight display.

4 Conclusions

In summary, we have discovered the novel Mn^{2+} -based narrow-band green-emitting Cs_3MnBr_5 Phosphor with $\lambda_{\text{em}} = 520$ nm, FWHM = 42 nm, and the luminescence originates from the intrinsic Mn^{2+} characteristic emission with abnormal short fluorescence lifetime value in the separated $[\text{MnBr}_4]$ tetrahedrons without concentration quenching. The thermal stability of Cs_3MnBr_5 is improved from 82% to 87% at 423 K by introducing a small amount of Zn^{2+} into Cs_3MnBr_5 . By combining $\text{Cs}_3\text{Mn}_{0.96}\text{Zn}_{0.04}\text{Br}_5$ green phosphor, $\text{KSF}:\text{Mn}^{4+}$ red phosphor and blue InGaN chips, the fabricated LED device shows the high luminous efficiency up to 107.66 lm/W with wide color gamut of 101 % NTSC for backlight display, which is larger than that of white LED based on commercial green phosphor $\beta\text{-SiAlON}:\text{Eu}^{2+}$ (89%). All results indicated that Cs_3MnBr_5 and $\text{Cs}_3\text{Mn}_{0.96}\text{Zn}_{0.04}\text{Br}_5$ phosphors can act as a promising narrow-band emitting green phosphor in the field of wide-color-gamut LCD backlight display.

Conflicts of interest

The authors declare no conflicts of interest.

Acknowledgements

The present work was supported by the National Natural Science Foundations of China (Grant No. 51722202, 91622125 and 51572023), Natural Science Foundations of Beijing (2172036), and the Guangdong Provincial Science & Technology Project (No. 2018A050506004).

References

- Z. G. Xia and Q. L. Liu, *Prog. Mater. Sci.*, 2016, **84**, 59-117.
- J. Zhou, Q. L. Liu and Z. G. Xia, *J. Mater. Chem. C*, 2018, **6**, 4371-4383.

- P. Pust, V. Weiler, C. Hecht, A. Tucks, A. S. Wochnik, A. K. Hens, D. Wiechert, C. Scheu, P. J. Schmidt and W. Schnick, *Nat. Mater.*, 2014, **13**, 891-896.
- L. Wang, X. Wang, T. Kohsei, K. Yoshimura, M. Izumi, N. Hirosaki and R. J. Xie, *Opt. Express*, 2015, **23**, 28707-28717.
- P. Pust, P. J. Schmidt and W. Schnick, *Nat. Mater.*, 2015, **14**, 454-458.
- N. Hirosaki, R. J. Xie, K. Kimoto, T. Sekiguchi, Y. Yamamoto, T. Suehiro and M. Mitomo, *Appl. Phys. Lett.*, 2005, **86**, 211905.
- S. Li, L. Wang, D. Tang, Y. Cho, X. Liu, X. Zhou, L. Lu, L. Zhang, T. Takeda, N. Hirosaki and R. J. Xie, *Chem. Mater.*, 2017, **30**, 494-505.
- X. J. Zhang, H. C. Wang, A. C. Tang, S. Y. Lin, H. C. Tong, C. Y. Chen, Y. C. Lee, T. L. Tsai and R. S. Liu, *Chem. Mater.*, 2016, **28**, 8493-8497.
- Z. C. Li, L. Kong, S. Q. Huang and L. Li, *Angew. Chem. Int. Edit.*, 2017, **56**, 8134-8138.
- H. C. Wang, S. Y. Lin, A. C. Tang, B. P. Singh, H. C. Tong, C. Y. Chen, Y. C. Lee, T. L. Tsai and R. S. Liu, *Angew. Chem. Int. Edit.*, 2016, **55**, 7924-7929.
- P. Strobel, S. Schmiechen, M. Siegert, A. Tücks, P. J. Schmidt and W. Schnick, *Chem. Mater.*, 2015, **27**, 6109-6115.
- T. Takeda, N. Hirosaki, S. Funahshi and R. J. Xie, *Chem. Mater.*, 2015, **27**, 5892-5898.
- M. Zhao, H. X. Liao, L. X. Ning, Q. Y. Zhang, Q. L. Liu and Z. G. Xia, *Adv. Mater.*, 2018, **30**, 1802489.
- H. X. Liao, M. Zhao, Y. Y. Zhou, M. S. Molokeev, Q. L. Liu, Q. Y. Zhang and Z. G. Xia, *Adv. Funct. Mater.*, 2019, 1901988.
- Q. Dong, F. L. Yang, J. Cui, Y. B. Tian, S. F. Liu, F. Du, J. Q. Peng and X. Y. Ye, *Ceram. Int.*, 2019, **45**, 11868-11875.
- E. H. Song, Y. Y. Zhou, Y. Wei, X. X. Han, Z. R. Tao, R. L. Qiu, Z. G. Xia and Q. Y. Zhang, *J. Mater. Chem. C*, 2019.
- Y. L. Zhu, Y. J. Liang, S. Q. Liu, H. R. Li and J. H. Chen, *Adv. Opt. Mater.*, 2019, **7**, 1801419.
- S. Zhang, H. B. Liang, Y. W. Liu, Y. F. Liu, D. J. Hou, G. B. Zhang and J. Y. Shi, *Opt. Lett.*, 2012, **37**, 2511-2513.
- V. Topas, *Bruker AXS, Karlsruhe, Germany*, 2008.
- D. Palumbo and J. Brown, *J. Electrochem. Soc.*, 1970, **117**, 1184-1188.
- G. Blasse and B. C. Grabmaier, in *Luminescent Materials*, Springer, Berlin, 1994.
- U. Caldiño, A. Lira, A. N. Meza Rocha, I. Camarillo and R. Lozada Morales, *J. Lumin.*, 2018, **194**, 231-239.
- E. H. Song, Y. Y. Zhou, Y. Wei, X. X. Han, Z. R. Tao, R. L. Qiu, Z. G. Xia and Q. Y. Zhang, *J. Mater. Chem. C*, 2019, DOI: 10.1039/c9tc02107h.
- J. H. Li, Q. Y. Liang, Y. F. Cao, J. Yan, J. B. Zhou, Y. Q. Xu, L. Dolgov, Y. Y. Meng, J. X. Shi and M. M. Wu, *ACS Appl. Mater. Interfaces*, 2018, **10**, 41479-41486.
- H. X. Liao, M. Zhao, M. S. Molokeev, Q. L. Liu and Z. G. Xia, *Angew. Chem. Int. Edit.*, 2018, **57**, 11728-11731.

Electronic supplementary information

Mn²⁺-Based Narrow-Band Green-Emitting Cs₃MnBr₅ Phosphor and the performance optimization by Zn²⁺ alloying

Binbin Su^a, Maxim Molokeev^{cde}, Zhiguo Xia^{*a}

a. State Key Laboratory of Luminescent Materials and Devices and Institute of Optical Communication Materials, South China University of Technology, Guangzhou 510641, China.

b. Laboratory of Crystal Physics, Kirensky Institute of Physics, Federal Research Center KSC SB RAS, Krasnoyarsk 660036, Russia

c. Siberian Federal University, Krasnoyarsk 660041, Russia

d. Department of Physics, Far Eastern State Transport University, Khabarovsk 680021 Russia

Table 1. Main parameters of processing and refinement of the Cs₃MnBr₅ sample

Compound	Cs ₃ MnBr ₅
Sp.Gr.	<i>I4/mcm</i>
<i>a</i> , Å	9.60672 (13)
<i>c</i> , Å	15.5716 (2)
<i>V</i> , Å ³	1437.08 (4)
<i>Z</i>	2
2θ-interval, °	10-105
<i>R</i> _{wp} , %	5.13
<i>R</i> _p , %	3.84
<i>R</i> _{exp} , %	2.31
χ ²	2.21
<i>R</i> _B , %	3.08

Table S2. Fractional atomic coordinates and isotropic displacement parameters (Å²) of Cs₃MnBr₅

	<i>x</i>	<i>y</i>	<i>z</i>	<i>B</i> _{iso}
Cs1	0.16040 (14)	0.66040 (14)	0.5	2.5 (2)
Cs2	0	0	0.25	3.0 (2)
Mn1	0	0.5	0.25	1.3 (3)
Br1	0.14742 (16)	0.64742 (16)	0.15389 (11)	3.0 (2)
Br2	0	0	0	2.3 (2)

Table S3. Main bond lengths (Å) of Cs₃MnBr₅

Cs1—Br1 ⁱ	3.8082 (19)	Cs2—Br1 ^{iv}	3.9646 (16)
Cs1—Br1 ⁱⁱ	3.5439 (19)	Cs2—Br2	3.8929 (1)
Cs1—Br2 ⁱⁱⁱ	3.6080 (13)	Mn1—Br1	2.5002 (16)

Symmetry codes: (i) $-x, y, -z+1/2$; (ii) $-y+1, -x+1, -z+1/2$; (iii) $-x, y+1, -z+1/2$; (iv) $x, y-1, z$; (v) $-x, y, z+1/2$.

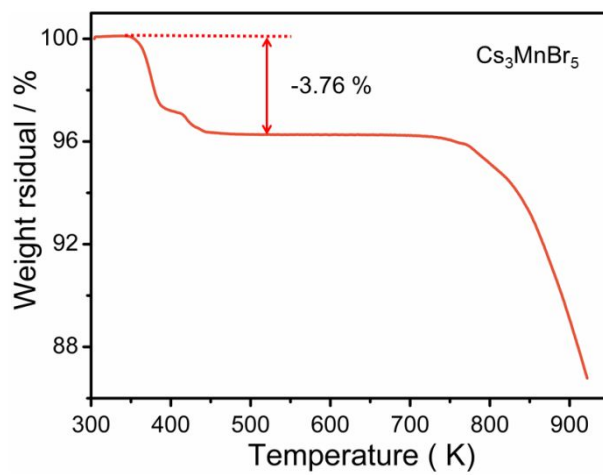


Fig. S1 The TG curve of Cs_3MnBr_5 sample.